

The Hartley transform in seismic imaging

Henning Kühl*, Maurico D. Sacchi*, and Jürgen Fertig‡

ABSTRACT

Phase-shift migration techniques that attempt to account for lateral velocity variations make substantial use of the fast Fourier transform (FFT). Generally, the Hermitian symmetry of the complex-valued Fourier transform causes computational redundancies in terms of the number of operations and memory requirements. In practice a combination of the FFT with the well-known real-to-complex Fourier transform is often used to avoid such complications. As an alternative means to the Fourier transform, we introduce the inherently real-valued, non-symmetric Hartley transform into phase-shift migration techniques. By this we automatically avoid the Hermitian symmetry resulting in an optimized algorithm that is comparable in efficiency to algorithms based on the real-to-complex FFT. We derive the phase-shift operator in the Hartley domain for migration in two and three dimensions and formulate phase shift plus interpolation, split-step migration, and split-step double-square-root prestack migration in terms of the Hartley transform as examples.

We test the Hartley phase-shift operator for poststack and prestack migration using the SEG/EAGE salt model and the Marmousi data set, respectively.

INTRODUCTION

Recursive phase-shift methods in seismic imaging are based on the use of the fast Fourier transform (FFT). For the feasibility of techniques such as phase shift (Gazdag, 1978), phase shift plus interpolation (PSPI) (Gazdag and Squazzero, 1984), and split-step migration (Stoffa et al., 1990), an efficient computer implementation, especially in 3-D and/or prestack migration, is important. Since the seismic wavefield is real valued, the complex Fourier transform has Hermitian symmetry. Hence, a brute force implementation leads to redundant operations and memory allocation. The combination of the complex FFT with a well-known modification of the FFT, the real-to-complex

FFT (Press et al., 1997), is often used to circumvent these redundancies.

Alternatively, the Hartley transform (Bracewell, 1986) can optimize such codes. The fast Hartley transform (FHT) is closely related to the complex FFT but is computationally more suitable for real data because of its inherently real-valued nature. The Hartley transform codes the amplitude and phase of a real function in a single, real-valued transform without symmetries. It satisfies similar theorems equivalent to those of the Fourier transform and can therefore replace the FFT in virtually any application that involves real-valued data (Bracewell, 1986). The Hartley transform has been used successfully in other applications such as wavefield modeling and data filtering (Saatcilar et al., 1990; Saatcilar and Ergintav, 1991).

A complete set of FHT algorithms is available in the literature. We exclusively deal with the radix-2, decimation-in-time FHT. We refer to Sorensen et al. (1985) for other implementations of the FHT.

To illustrate the use of the Hartley transform in seismic imaging, we pose the phase-shift wavefield extrapolator in the Hartley domain and provide flowcharts and migration examples for the derived algorithms.

THE HARTLEY TRANSFORM

The 1-D Hartley transform and its inverse are given by

$$H(u) = \frac{1}{\sqrt{2\pi}} \int f(x) \text{cas}(ux) dx,$$

$$f(x) = \frac{1}{\sqrt{2\pi}} \int H(u) \text{cas}(ux) du, \quad (1)$$

with the real-valued Hartley kernel $\text{cas}(ux) = \cos(ux) + \sin(ux)$ (Bracewell, 1986). The orthogonal Hartley transform is related to the unitary Fourier transform and satisfies similar theorems. For seismic imaging an extension of definition (1) to higher dimensions becomes necessary. This extension is not obvious since

$$\text{cas}(ux + vy) \neq \text{cas}(ux) \text{cas}(vy), \quad (2)$$

as opposed to the Fourier kernel, which is separable:

Manuscript received by the Editor August 12, 1999; revised manuscript received October 26, 2000.

*University of Alberta, Department of Physics, Edmonton, AB T6G 2J1, Canada. E-mail: hkuehl@phys.ualberta.ca; msacchi@phys.ualberta.ca.

‡Technische Universität Clausthal, Institut für Geophysik, 38678 Clausthal-Zellerfeld, Germany. E-mail: juergen.fertig@tu-clausthal.de.

© 2001 Society of Exploration Geophysicists. All rights reserved.

$$\exp(i(ux + vy)) = \exp(iux) \exp(ivy). \quad (3)$$

Both sides of equation (2) are used as 2-D Hartley kernels in the literature. Here, we adopt the multiplicative definition of the 2-D Hartley transform suggested by Sundarajan (1995) and refer to it as version I:

$$H_I(u, v) = \frac{1}{2\pi} \iint f(x, y) \operatorname{cas}(ux) \operatorname{cas}(vy) dx dy, \quad (4)$$

with an obvious extension to the 3-D case:

$$H_I(u, v, w) = \frac{1}{(2\pi)^{\frac{3}{2}}} \iiint f(x, y, z) \operatorname{cas}(ux) \operatorname{cas}(vy) \times \operatorname{cas}(wz) dx dy dz. \quad (5)$$

Some authors refer to this definition as the *cas*(*cas*) transform (e.g., Bracewell, 1986). For stylistic reasons we call equations (4) and (5) (multidimensional) Hartley transforms (version I), in agreement with Sundarajan (1995). Sundarajan also defines version II of the 2-D Hartley transform:

$$H_{II}(u, v) = \frac{1}{2\pi} \iint f(x, y) \operatorname{cas}(ux + vy) dx dy, \quad (6)$$

where the argument of the kernel is the sum of the arguments of the 1-D kernels. However, definitions (4) and (5) are separable into 1-D Hartley transforms and therefore are computationally more convenient to obtain than version II. Both versions of the N -dimensional Hartley transform are orthogonal.

FAST HARTLEY TRANSFORM

In accordance with equation (1), the discrete 1-D Hartley transform (DHT) and its inverse for a length- N sequence $f(n)$, $0 \leq n \leq N-1$, are defined by (Bracewell, 1986)

$$H(v) = \sum_{n=0}^{N-1} f(n) \operatorname{cas}\left(\frac{2\pi}{N}vn\right), \quad 0 \leq v \leq N-1,$$

$$f(n) = \frac{1}{N} \sum_{v=0}^{N-1} H(v) \operatorname{cas}\left(\frac{2\pi}{N}vn\right), \quad 0 \leq n \leq N-1. \quad (7)$$

A complete set of fast algorithms for computing the DHT is given by Sorensen et al. (1985), including a radix-2, decimation-in-time FHT. The decimation-in-time FHT is based on the Danielson–Lanczos formula for the discrete Fourier transform (DFT) (Press et al., 1997). A length $N = 2^M$ DHT is divided into two length- $N/2$ DHTs—one over the even-indexed samples (H_{even}) and one over the odd-indexed samples (H_{odd})—and combined to form the DHT of the full-length sequence:

$$H(v) = H_{\text{even}}(v) + H_{\text{odd}}(v) \cos\left(\frac{2\pi}{N}v\right) + H_{\text{odd}}(N-v) \sin\left(\frac{2\pi}{N}v\right), \quad 0 \leq v \leq N-1, \quad (8)$$

where the indices of the half-length transforms for the even and odd indices are evaluated modulo $N/2$. The decomposition formula (8) is applied recursively until length-2 transforms are

obtained. This structure resembles the FFT derived by Cooley and Tukey (1965). Figure 1 shows a flowchart representation of equation (8), called the (Hartley butterfly). Since we want to compute the FHT in place, four elements are included in each Hartley butterfly to avoid overwriting an element that will be needed later. Sorensen et al. (1985) provide a radix-2, decimation-in-time FHT Fortran code based on the described Hartley butterfly. They also conduct a number-of-operations count and show that, when coded efficiently, the FHT takes only a few more additions than an equivalent real-to-complex FFT. In this sense the FHT can be regarded as a means to compute a time- and memory-optimized, real-valued spectral transform. The extension to higher dimensions (version I) is most easily accomplished by multiple application of the 1-D FHT along the respective dimensions without loss in efficiency.

However, we do not suggest that algorithms based on the Hartley transform are generally more efficient than those using the real-to-complex FFT. We merely propose the Hartley transform as an alternative tool that might be attractive to practitioners developing efficient algorithms which exploit the symmetries of the Fourier transform.

PHASE-SHIFT MIGRATION USING HARTLEY TRANSFORM

The 2-D phase-shift, zero-offset migration for stratified media down to depth z is expressed as (Gazdag, 1978)

$$P(k_x, z, t = 0) = \frac{1}{\sqrt{2\pi}} \int P(k_x, z = 0, \omega) e^{i \sum_j k_{zj} j(k_x, \omega) \Delta z} d\omega, \quad (9)$$

where $P(k_x, z = 0, \omega)$ is the 2-D Fourier transform of the seismic wavefield $P(x, z = 0, t)$ recorded at the surface of the earth:

$$P(k_x, z = 0, \omega) = \frac{1}{2\pi} \iint P(x, z = 0, t) e^{-i(k_x x + \omega t)} dx dt. \quad (10)$$

The variables x and t are the surface and time coordinates, and k_x and ω are their respective Fourier counterparts. The vertical wavenumber k_{zj} in the individual extrapolation step from depth z_j to $z_j + \Delta z$,

$$P(k_x, z_j + \Delta z, \omega) = P(k_x, z_j, \omega) e^{i k_{zj} j(k_x, \omega) \Delta z}, \quad (11)$$

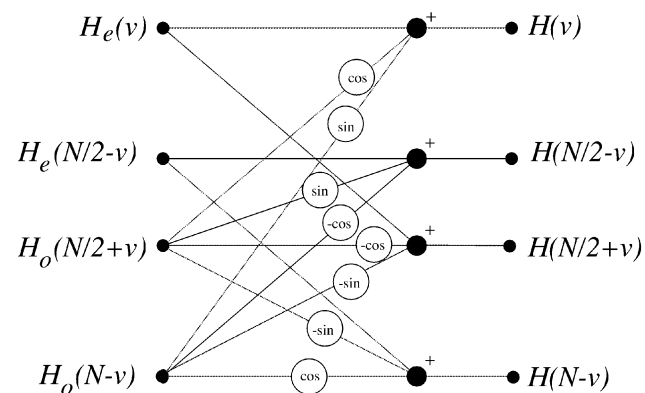


FIG. 1. The Hartley butterfly according to equation (8). The sine and cosine factors are evaluated at $(2\pi/N)v$, where N is the length of the discrete sequence.

is given by the dispersion relation for the downgoing one-way acoustic-wave equation:

$$k_{z_j} = \frac{\omega}{v(z_j)} \sqrt{1 - \left(\frac{v(z_j)k_x}{\omega} \right)^2}, \quad (12)$$

where $v(z_j)$ is the velocity in the j th layer of thickness Δz . The wavefield is recursively downward continued (extrapolated) by successive applications of the phase-shift operator (11). In doing so, the imaging principle for zero-offset data is applied at each depth step Δz by summing over the frequencies ω .

In the Appendix we derive the analog to the Fourier phase-shift operator (11) in terms of the Hartley transform:

$$\begin{aligned} P_{\mathcal{H}_I}(k_x, z_j + \Delta z, \omega) &= P_{\mathcal{H}_I}(k_x, z_j, \omega) \cos(k_{z_j} \Delta z) \\ &- P_{\mathcal{H}_I}(-k_x, z_j, \omega) \sin(k_{z_j} \Delta z), \end{aligned} \quad (13)$$

where \mathcal{H}_I denotes the version I 2-D Hartley transform over x and t . Instead of one complex multiplication, two real multiplications must be carried out. The wavenumber k_x appears mirrored with respect to the ω -axis in the second term of equation (13). Substituting the Fourier transform by the Hartley transform and equation (11) by equation (13) yields the phase-shift scheme in the Hartley domain.

Gazdag's phase-shift migration is known for its computational efficiency. However, the major drawback of this technique lies in its restriction to media with laterally constant velocities. Correction techniques like phase-shift plus interpolation and split-step migration that attempt to compensate for lateral velocity variations make additional Fourier/Hartley transforms at each depth step Δz necessary.

PHASE SHIFT PLUS INTERPOLATION USING HARTLEY TRANSFORM

Gazdag and Squazzero (1984) propose the phase shift plus interpolation (PSPI) technique to account for lateral velocity variations. The extrapolation procedure consists essentially of two steps. First, the wavefield is downward continued over a depth step Δz using a number of constant velocities. Second, the actual wavefield is computed by interpolating the resulting reference wavefields. The interpolation step makes one additional Fourier/Hartley transform per depth step and reference wavefield inevitable. The concept of PSPI is not altered by the number of reference velocities and is demonstrated here for two velocities.

To avoid distortion of zero-dip reflectors, the extrapolation step is split into two operations. A correction term is applied prior to the spatial Fourier transform,

$$\tilde{P}(x, z_j, \omega) = P(x, z_j, \omega) e^{i \frac{\omega}{v(x, z_j)} \Delta z}, \quad (14)$$

followed by the phase-shift term applied to the wavefield for a constant reference velocity $v'(z_j)$:

$$P(k_x, z_j + \Delta z, \omega) = \tilde{P}(k_x, z_j, \omega) e^{i(k_{z_j}' - \frac{\omega}{v'}) \Delta z}, \quad (15)$$

where $\min\{v(x, z_j)\} \leq v'(z_j) \leq \max\{v(x, z_j)\}$. For flat reflectors, $k_x = 0$, the phase in equation (15) is zero and the reflectors are therefore downward continued with the correct velocities $v(x, z_j)$ by equation (14).

The first step [equation (14)] is a time shift applied to each trace and can be accomplished in the Hartley domain by replacing equation (14) with the corresponding time-shift theorem for the Hartley transform (Bracewell, 1986):

$$\begin{aligned} \tilde{P}_{\mathcal{H}_I}(x, z_j, \omega) &= P_{\mathcal{H}_I}(x, z_j, \omega) \cos\left(\frac{\omega}{v(x, z_j)} \Delta z\right) \\ &- P_{\mathcal{H}_I}(x, z_j, -\omega) \sin\left(\frac{\omega}{v(x, z_j)} \Delta z\right). \end{aligned} \quad (16)$$

According to equation (13), the second step is the Hartley phase-shift operator with the incorporated correction term $(\omega/v')\Delta z$:

$$\begin{aligned} P_{\mathcal{H}_I}(k_x, z_j + \Delta z, \omega) &= \tilde{P}_{\mathcal{H}_I}(k_x, z_j, \omega) \cos\left(\left(k_{z_j}' - \frac{\omega}{v'}\right) \Delta z\right) \\ &- \tilde{P}_{\mathcal{H}_I}(-k_x, z_j, \omega) \sin\left(\left(k_{z_j}' - \frac{\omega}{v'}\right) \Delta z\right). \end{aligned} \quad (17)$$

Finally, the Hartley coefficients $P_{\mathcal{H}_I}^1(k_x, z_j + \Delta z, \omega)$ and $P_{\mathcal{H}_I}^2(k_x, z_j + \Delta z, \omega)$, downward continued using the reference velocities v_1 and v_2 , are interpolated in space:

$$\begin{aligned} P_{\mathcal{H}_I}(x, z_j + \Delta z, \omega) &= \\ \frac{P_{\mathcal{H}_I}^1(x, z_j + \Delta z, \omega)(v_2 - v) + P_{\mathcal{H}_I}^2(x, z_j + \Delta z, \omega)(v - v_1)}{v_2 - v_1}. \end{aligned} \quad (18)$$

The flowchart representation for PSPI in terms of the Hartley transform is shown in Figure 2. Except for the reference wavefields that need to be stored temporarily, all computations are carried out in place.

SPLIT-STEP MIGRATION USING HARTLEY TRANSFORM

Split-step migration (Stoffa et al., 1990) is an interesting alternative to PSPI that also partially accounts for lateral velocity variations but does not use reference wavefields and requires only one additional Fourier/Hartley transform pair per depth step. This makes split-step migration especially attractive for the migration of 3-D data sets and prestack migration. Split-step migration is originally derived directly from a variable velocity wave equation as a first-order approximation to the one-way acoustic wave equation.

Split-step migration in two dimensions

The split-step scheme is expressed in terms of the slowness perturbation $\Delta u(x, z_j) = u(x, z_j) - \bar{u}(z_j)$, where $\bar{u}(z_j) = 1/\bar{v}(z_j)$ is the mean slowness of the layer at depth z_j . First, the wavefield is extrapolated using $\bar{u}(z_j)$:

$$\tilde{P}(k_x, z_j, \omega) = P(k_x, z_j, \omega) e^{i k_{z_j} \Delta z}, \quad (19)$$

where

$$k_{z_j} = \omega \bar{u}(z_j) \sqrt{1 - \frac{k_x^2}{\bar{u}^2(z_j) \omega^2}}. \quad (20)$$

Second, each trace is individually time-shifted according to the slowness perturbation $\Delta u(x, z_j)$:

$$P(x, z_j + \Delta z, \omega) = \tilde{P}(x, z_j, \omega) e^{i \omega \Delta u(x, z_j) \Delta z}. \quad (21)$$

Following the concept outlined for PSPI, the transfer to the Hartley domain is evident, as illustrated in Figure 3.

Split-step migration in three dimensions

The form of the 3-D Hartley phase-shift operator differs from the 2-D case and is derived in the Appendix, yielding the following analog to equation (19):

$$\begin{aligned} \tilde{P}_{\mathcal{H}_I}(k_x, k_y, z, \omega) &= P_{\mathcal{H}_I}(k_x, k_y, z, \omega) \cos(k_{z_j} \Delta z) \\ &\quad - P_{\mathcal{H}_I}(k_x, k_y, z, -\omega) \sin(k_{z_j} \Delta z). \end{aligned} \quad (22)$$

The dispersion relation for the one-way wave equation is now written for three dimensions as

$$k_{z_j} = \omega \bar{u}(z_j) \sqrt{1 - \frac{k_x^2 + k_y^2}{\bar{u}^2(z_j) \omega^2}}, \quad (23)$$

where k_y is the wavenumber for the additional spatial y-coordinate of the 3-D data set.

Split-step DSR prestack migration

Knowing the Hartley phase-shift operator in three dimensions makes implementing split-step, double-square-root

(DSR) prestack migration (Popovici, 1996) in the Hartley domain straightforward. The spatial dimensions x, y in equation (22) become midpoint and offset coordinates, respectively, and the dispersion relation (23) is replaced by the DSR equation (Claerbout, 1985). Following Popovici (1996), the complete split-step DSR algorithm in terms of the Hartley transform is summarized in Figure 4.

EXAMPLES

SEG/EAGE salt model and Marmousi data set

We have tested our PSPI and split-step poststack migration with an exploding reflector data set based on the SEG/EAGE salt model (O'Brien and Gray, 1996) and the split-step DSR prestack migration with the Marmousi data set (Bourgeois et al., 1991).

The PSPI and split-step migrated sections for the salt model using the Hartley transform are depicted in Figure 5. Overall, the PSPI migration produces a much better imaging result than the faster split-step migration. However, the PSPI method shows slight deficiencies for the steep salt flanks, and not all of the steep faults in the subsalt zone are properly imaged. Clearly, PSPI is sensitive to the reference velocities, and a higher number of them will result in a more accurate image. To select the velocities at each depth step, we used the adaptive algorithm of Bagaini et al. (1995), averaging 5.7 reference velocities per depth step.

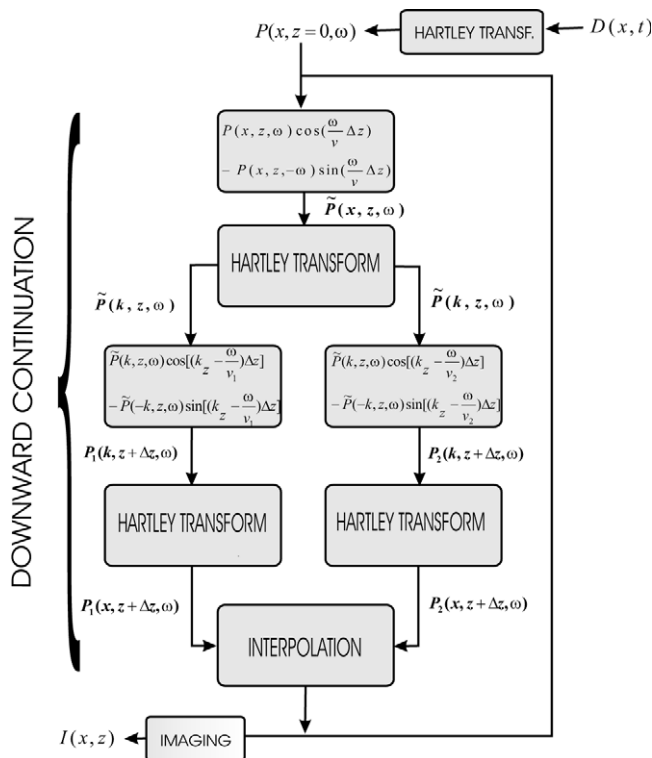


FIG. 2. Representation of PSPI migration using the Hartley transform. The seismic data $P(x, z = 0, t) = D(x, t)$ are recursively downward-continued to depth z in steps Δz using multiple reference velocities. In the diagram the PSPI concept is illustrated for two reference velocities. The migrated image $I(x, z)$ is obtained by summing over the frequencies of $\tilde{P}(x, z, \omega)$.

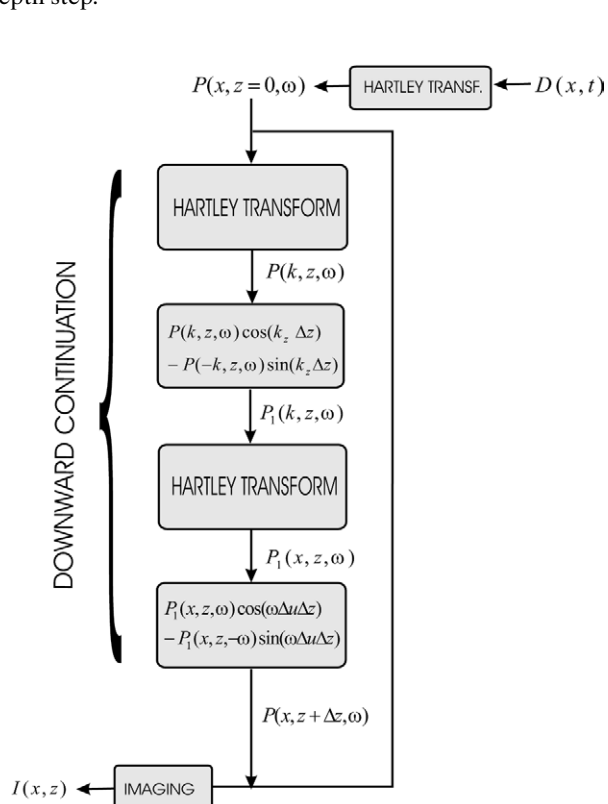


FIG. 3. Representation of split-step migration using the Hartley transform. The seismic data $P(x, z = 0, t) = D(x, t)$ are recursively downward-continued to depth z in steps Δz . The migrated image $I(x, z)$ is obtained by summing over the frequencies of $P(x, z, \omega)$.

The migration of the Marmousi data set and the underlying velocity model is shown in Figure 6. As previously shown by Popovici (1996), the split-step DSR algorithm gives an excellent image of the Marmousi model.

Kessinger (1992) introduces the multiple-reference slowness logic of the PSPI method in the split-step technique to increase its accuracy. Ristow and Rühl (1994) present a modification to the split-step method, introducing a finite-difference term in the downward-continuation operator. Margrave and Ferguson (1999) propose nonstationary phase-shift migration (NSPS) and demonstrate in synthetic examples that, in the presence of lateral velocity discontinuities, NSPS is superior to the PSPI operator. All these modifications are interesting, but a detailed study of them is beyond the scope of this paper. Our examples primarily confirm the equivalence between the Fourier and the Hartley methods in seismic imaging in general. For a more systematic comparison of the various migration techniques based on the Marmousi model, refer to Han (1996).

We have implemented our codes on an SGI Origin 2400 shared-memory parallel computer (400-MHz processors). The algorithms have been parallelized with respect to the frequencies. For the migration of the Marmousi data, every second midpoint was used, resulting in a midpoint-offset data set of size $256 \times 64 \times 1024$ (including zero padding for the FHT). The migration was performed for a frequency band of 5 to 60 Hz and took about 70 s on 32 processors.

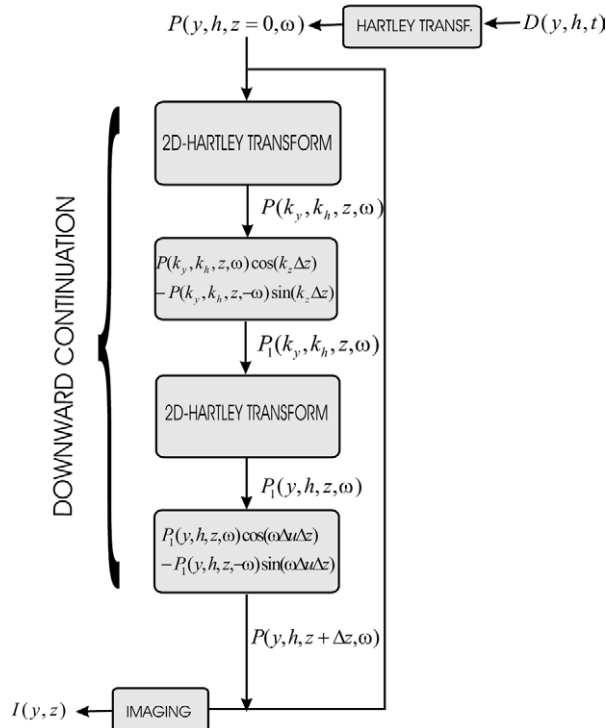


FIG. 4. Representation of split-step DSR prestack migration using the Hartley transform. The prestack data $P(y, h, z=0, t) = D(y, h, z=0, t)$ in midpoint-offset coordinates are recursively downward-continued to depth z in steps Δz . The migrated image $I(y, z)$ is obtained by evaluating the wavefield $P(y, h, z, \omega)$ in the frequency domain at offset $h=0$ and by summing over ω .

CONCLUSIONS

We have introduced the Hartley transform into seismic imaging based on recursive wavefield extrapolators by posing phase-shift, PSPI, and DSR migration in the Hartley domain. To accomplish this, we derived the corresponding phase-shift operator in the 2-D and 3-D Hartley domains. Similar to algorithms based on the real-to-complex FFT, the resulting Hartley algorithms avoid the computational inefficiency caused by the

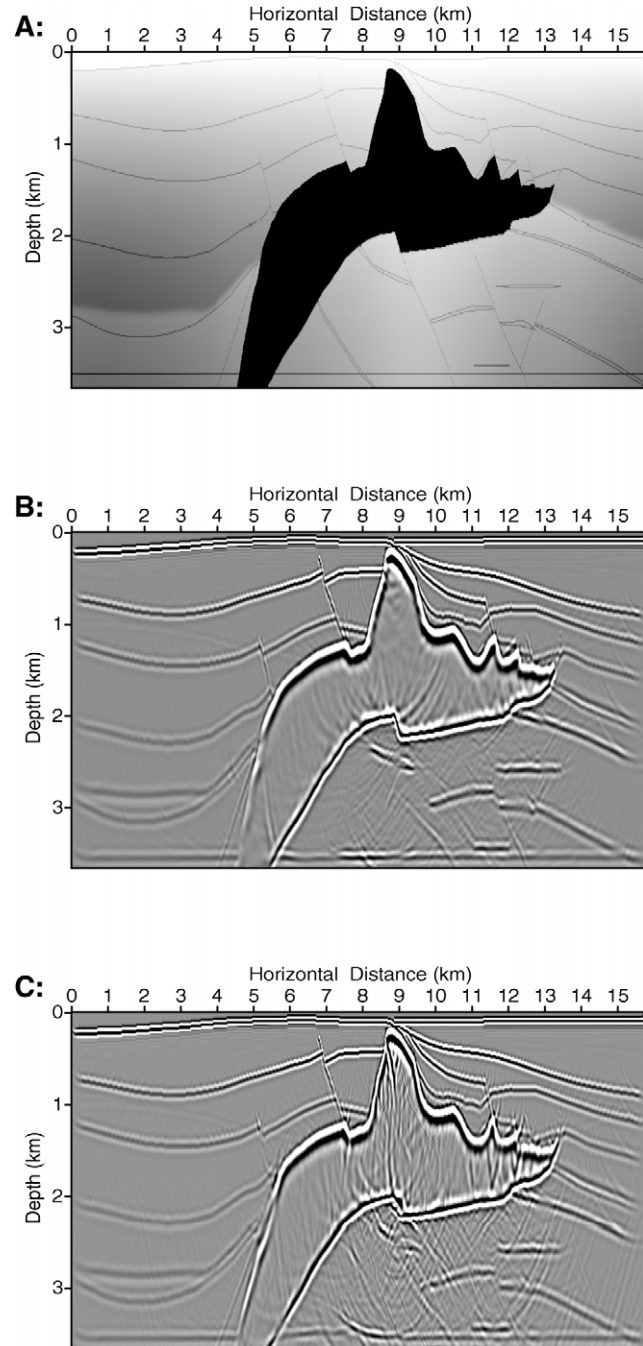


FIG. 5. (A) Profile A–A' from the SEG/EAGE salt model. The velocities range from 1500 to 4500 m/s. Darker shades denote higher velocities. (B) PSPI migration using 5.7 reference velocities per depth step on average. (C) Split-step migration.

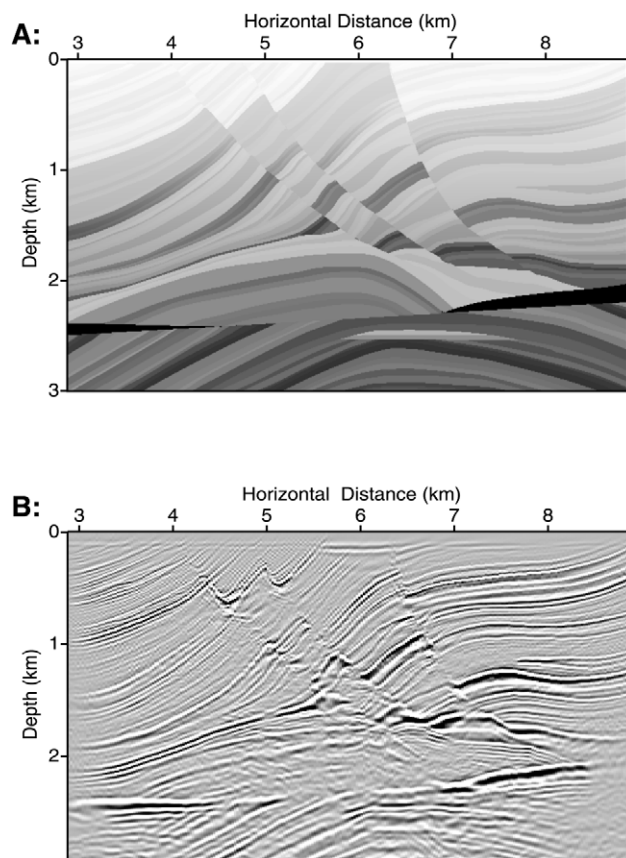


FIG. 6. (A) Marmousi velocity model. The velocities range from 1500 to 5500 m/s. Darker shades denote higher velocities. (B) Split-step DSR prestack migration.

Hermitian symmetry of the complex FFT. The Hartley algorithms are straightforward to implement and efficient in computation time and memory requirements. Tests based on the SEG/EAGE salt model and the Marmousi model confirm the mathematical equivalence of the Hartley migration algorithms to their Fourier counterparts.

The parallel implementation in a shared-memory multiprocessor architecture can reduce the cost of prestack split-step migration for data sets such as the Marmousi data to the order of 1 minute.

ACKNOWLEDGMENTS

We appreciate the valuable comments and suggestions from reviewers Brian Sumner and Chuck Mosher and associate editor Craig Artley. We thank Amoco Production Co. for providing the data for the SEG/EAGE salt model. This research was partially funded by Pan Canadian Petroleum Ltd., Geo-X Ltd., Veritas and a grant from the Natural Sciences and Engineering Research Council of Canada. We are grateful for their financial support.

REFERENCES

- Bagaini, C., Bonomi, E., and Pieroni, E., 1995, Data parallel implementation of 3-D PSPI: 65th Ann. Internat. Mtg., Soc. Expl. Geophys., Expanded Abstracts, 188–191.
- Bourgeois, A., Bourget, M., Lailly, P., Poulet, M., Ricarte, P., and Versteeg, R., 1991, Marmousi, model and data: Practical Aspects of Seismic Data Inversion, Eur. Assn. Geosci. Eng., Proceedings, Bracewell, R. N., 1986, The Hartley transform: Oxford Univ. Press, Inc.
- Bronstein, I. N., Semendjajew, K. A., Musiol, G., and Mühlig, H., 1997, Taschenbuch der mathematik: Verlag Harri Deutsch.
- Claerbout, J. F., 1985, Imaging the earth's interior: Blackwell Scientific Publications, Inc.
- Cooley, J. W., and Tukey, J. W., 1965, An algorithm for the machine calculation of complex Fourier series: Math. Comput., **19**, No. 2, 297–301.
- Gazdag, J., 1978, Wave equation migration with the phase shift method: Geophysics, **43**, 1342–1351.
- Gazdag, J., and Squazzero, P., 1984, Migration of seismic data by phase shift plus interpolation: Geophysics, **49**, 124–131.
- Han, B., 1996, A comparison of four depth-migration methods: 66th Ann. Internat. Mtg., Soc. Expl. Geophys., Expanded Abstracts, 1104–1107.
- Kessinger, W., 1992, Extended split-step Fourier migration: 62nd Ann. Internat. Mtg., Soc. Expl. Geophys., Expanded Abstracts, 917–920.
- Margrave, G. F., and Ferguson, R. J., 1999, Wavefield extrapolation by nonstationary phase shift: Geophysics, **64**, 1067–1078.
- O'Brien, M. J., and Gray, A. H., 1996, Can we image beneath salt?: The Leading Edge, **15**, No. 1, 17–22.
- Popovici, A. M., 1996, Prestack migration by split-step DSR: Geophysics, **61**, 1412–1416.
- Press, W. H., Flannery, B. P., Teukolsky, S. A., and Vetterling, W. T., 1997, Numerical recipes in C: Cambridge Univ. Press.
- Ristow, D., and Rühl, T., 1994, Fourier finite-difference migration: Geophysics, **59**, 1882–1893.
- Saatçilar, R., and Ergintav, S., 1991, Solving the elastic wave equations with the Hartley transform method: Geophysics, **56**, 274–278.
- Saatçilar, R., Ergintav, S., and Canitez, N., 1990, The use of the Hartley transform in geophysical applications: Geophysics, **55**, 1488–1495.
- Sorensen, H. V., Jones, D. L., Burrus, S., and Heideman, M. T., 1985, On computing the discrete Hartley transform: IEEE Trans. Acoust. Speech Sig. Proc., **ASSP-33**, 1231–1238.
- Stoffa, P. L., Fokkema, J. T., de Luna Freire, R. M., and Kessinger, W. P., 1990, Split-step Fourier migration: Geophysics, **55**, 410–421.
- Sundarajan, N., 1995, 2-D Hartley transforms: Geophysics, **60**, 262–267.

APPENDIX

PHASE-SHIFT OPERATOR IN HARTLEY DOMAIN

To avoid notational clutter, we denote the extrapolated wavefield by a prime, $P'_H(k_x, k_y, \omega) = P_H(k_x, k_y, z_j + \Delta z, \omega)$, and use the subscripts $P_{\mathcal{H}_I}$ and $P_{\mathcal{H}_{II}}$ to differentiate between the Hartley-transformed wavefields according to versions I and II, respectively.

Phase-shift operator for 2-D Hartley transform (version I)

We express the 2-D Hartley transform (version I) as the sum of its even part $E_{\mathcal{H}_I}(k_x, \omega)$ and its odd part $O_{\mathcal{H}_I}(k_x, \omega)$:

$$\begin{aligned} E_{\mathcal{H}_I}(k_x, \omega) &= \frac{1}{2}[P_{\mathcal{H}_I}(k_x, \omega) + P_{\mathcal{H}_I}(-k_x, -\omega)] \\ &= \frac{1}{2\pi} \iint P(x, t) \cos(k_x x - \omega t) dx dt, \quad (\text{A-1}) \end{aligned}$$

$$\begin{aligned} O_{\mathcal{H}_I}(k_x, \omega) &= \frac{1}{2}[P_{\mathcal{H}_I}(k_x, \omega) - P_{\mathcal{H}_I}(-k_x, -\omega)] \\ &= \frac{1}{2\pi} \iint P(x, t) \sin(k_x x + \omega t) dx dt. \quad (\text{A-2}) \end{aligned}$$

Comparison of the real part $R(k_x, \omega)$ and the imaginary part $I(k_x, \omega)$ of the Fourier transform (10) with equations (A-1) and (A-2) yields

$$\begin{aligned} E_{\mathcal{H}_I}(k_x, \omega) &= R(k_x, -\omega), \\ O_{\mathcal{H}_I}(k_x, \omega) &= -I(k_x, \omega). \quad (\text{A-3}) \end{aligned}$$

With $P'_{\mathcal{H}_I}(k_x, \omega) = E'_{\mathcal{H}_I}(k_x, \omega) + O'_{\mathcal{H}_I}(k_x, \omega)$, the relations (A-3), and the Fourier phase-shift operator (9), the Hartley domain phase-shift operator (version I) is found by direct substitution after a few algebraic steps:

$$\begin{aligned} P'_{\mathcal{H}_I}(k_x, \omega) &= P_{\mathcal{H}_I}(k_x, \omega) \cos(k_z \Delta z) \\ &\quad - P_{\mathcal{H}_I}(-k_x, \omega) \sin(k_z \Delta z). \quad (\text{A-4}) \end{aligned}$$

Phase-shift operator for 3-D Hartley transform (version I)

Given that version II of the 3-D Hartley transform satisfies

$$P_{\mathcal{H}_{II}}(k_x, k_y, \omega) = R(k_x, k_y, \omega) - I(k_x, k_y, \omega), \quad (\text{A-5})$$

we can easily find the corresponding phase-shift operator (version II):

$$\begin{aligned} P'_{\mathcal{H}_{II}}(k_x, k_y, \omega) &= P_{\mathcal{H}_{II}}(k_x, k_y, \omega) \cos(k_z \Delta z) \\ &\quad - P_{\mathcal{H}_{II}}(-k_x, -k_y, -\omega) \sin(k_z \Delta z). \quad (\text{A-6}) \end{aligned}$$

Using the addition formulas for cosine and sine in three dimensions (Bronstein et al., 1997), we derive the following relations between versions I and II of the Hartley transform in three dimensions:

$$\begin{aligned} P_{\mathcal{H}_{II}}(k_x, k_y, \omega) &= \frac{1}{2}[P_{\mathcal{H}_I}(-k_x, k_y, \omega) + P_{\mathcal{H}_I}(k_x, -k_y, \omega) \\ &\quad + P_{\mathcal{H}_I}(k_x, k_y, -\omega) - P_{\mathcal{H}_I}(-k_x, -k_y, -\omega)] \quad (\text{A-7}) \end{aligned}$$

and

$$\begin{aligned} P_{\mathcal{H}_I}(k_x, k_y, \omega) &= \frac{1}{2}[P_{\mathcal{H}_{II}}(-k_x, k_y, \omega) + P_{\mathcal{H}_{II}}(k_x, -k_y, \omega) \\ &\quad + P_{\mathcal{H}_{II}}(k_x, k_y, -\omega) \\ &\quad - P_{\mathcal{H}_{II}}(-k_x, -k_y, -\omega)], \quad (\text{A-8}) \end{aligned}$$

which means the same relation holds in both directions.

Noting that sine terms change their leading sign for negative frequencies to honor the Hermitian symmetry of the Fourier transform, relations (A-6), (A-7), and (A-8) are used to yield the phase-shift operator for the 3-D Hartley transform (version I):

$$\begin{aligned} P'_{\mathcal{H}_I}(k_x, k_y, \omega) &= \frac{1}{2}[P'_{\mathcal{H}_{II}}(-k_x, k_y, \omega) + P'_{\mathcal{H}_{II}}(k_x, -k_y, \omega) \\ &\quad + P'_{\mathcal{H}_{II}}(k_x, k_y, -\omega) \\ &\quad - P'_{\mathcal{H}_{II}}(-k_x, -k_y, -\omega)] \\ &= \frac{1}{2}[P_{\mathcal{H}_{II}}(-k_x, k_y, \omega) \cos(k_z \Delta z) \\ &\quad - P_{\mathcal{H}_{II}}(k_x, -k_y, -\omega) \sin(k_z \Delta z) \\ &\quad + P_{\mathcal{H}_{II}}(k_x, -k_y, \omega) \cos(k_z \Delta z) \\ &\quad - P_{\mathcal{H}_{II}}(-k_x, k_y, -\omega) \sin(k_z \Delta z) \\ &\quad + P_{\mathcal{H}_{II}}(k_x, k_y, -\omega) \cos(k_z \Delta z) \\ &\quad + P_{\mathcal{H}_{II}}(-k_x, -k_y, \omega) \sin(k_z \Delta z) \\ &\quad - P_{\mathcal{H}_{II}}(-k_x, -k_y, -\omega) \cos(k_z \Delta z) \\ &\quad - P_{\mathcal{H}_{II}}(k_x, k_y, \omega) \sin(k_z \Delta z)] \\ &= P_{\mathcal{H}_I}(k_x, k_y, \omega) \cos(k_z \Delta z) \\ &\quad - \frac{1}{2}[P_{\mathcal{H}_{II}}(k_x, -k_y, -\omega) \\ &\quad + P_{\mathcal{H}_{II}}(-k_x, k_y, -\omega) \\ &\quad - P_{\mathcal{H}_{II}}(-k_x, -k_y, \omega) \\ &\quad + P_{\mathcal{H}_{II}}(k_x, k_y, \omega)] \sin(k_z \Delta z) \\ &= P_{\mathcal{H}_I}(k_x, k_y, \omega) \cos(k_z \Delta z) \\ &\quad - P_{\mathcal{H}_I}(-k_x, -k_y, -\omega) \sin(k_z \Delta z) \\ &\quad - [P_{\mathcal{H}_{II}}(k_x, k_y, \omega) \\ &\quad - P_{\mathcal{H}_{II}}(-k_x, -k_y, \omega)] \sin(k_z \Delta z) \\ &= P_{\mathcal{H}_I}(k_x, k_y, \omega) \cos(k_z \Delta z) \\ &\quad - P_{\mathcal{H}_I}(k_x, k_y, -\omega) \sin(k_z \Delta z). \quad (\text{A-9}) \end{aligned}$$

The complex phase-shift term is replaced by two real multiplications in the Hartley domain.